Short-range order in Ni-8.4 at.% Au above the miscibility gap

M. J. Portmann,[1] B. Schönfeld,[1] G. Kostorz,[1] and F. Altorfer[2]
[1]*ETH Zürich, Institute of Applied Physics, CH-8093 Zürich, Switzerland*
[2]*Laboratory for Neutron Scattering, ETH Zürich and PSI, CH-5232 Villigen, Switzerland*
(Received 21 June 2001; published 19 December 2001)

The elastic diffuse neutron scattering was measured for a Ni-8.4 at.% Au single crystal above the miscibility gap at 1083 K. The Ni-58 isotope was used to reduce the incoherent scattering. In contrast to previous x-ray investigations, short-range order scattering reflects local atomic arrangements characteristic of decomposition. This can be uniequivocally concluded from the diffuse scattering within the first Brillouin zone. For larger scattering vectors, the diffuse scattering is dominated by the displacement scattering due to the large difference in atomic sizes. The magnitudes of the extracted Warren-Cowley short-range order parameters show a smooth decrease with increasing distance. Crystals modeled on the basis of these parameters reveal basic arrangements of small Au clusters consisting of a tetrahedron and an attached fifth Au atom. The effective pair interaction parameters obtained from an inverse Monte Carlo analysis give no hint for a metastable state with $L1_2$ structure.

DOI: 10.1103/PhysRevB.65.024110 PACS number(s): 61.66.Dk, 64.90.+b

I. INTRODUCTION

Ni-Au is a system with a large atomic size mismatch of 15%. At temperatures below the fcc solid-solution regime, a large asymmetric miscibility gap with a critical temperature of 1083 K is observed (Fig. 1).[1] For the microstructure of the solid solution, one might expect local decomposition as Ni-Au has a large positive energy of mixing. However, conflicting results[2–4] were reported for the microstructure of the solid solution employing diffuse x-ray scattering, a tool[5,6] that has yielded detailed information on the microstructure of many other alloys.

Flinn *et al.*[2] measured the diffuse x-ray scattering at 83 K from several polycrystalline Ni-Au alloys with Au contents between 10 and 70 at.%, after quenching from 1173 K. The analysis of diffuse scattering in terms of short-range order and linear displacements resulted in negative values of -0.02 to -0.04 for the nearest-neighbor short-range order parameter α_{110}, i.e., a tendency towards local order.

Wu and Cohen[3] investigated the microstructure of a Ni-60 at.% Au single crystal by three-dimensional diffuse x-ray scattering at 1023 K, about 30 K above the miscibility gap. Taking into account quadratic besides terms of linear-displacement scattering, a slightly positive value of α_{110} is obtained, i.e., a tendency towards local decomposition. Based on model crystals, the microstructure is characterized by compositional fluctuations consisting of Ni-rich regions on {100} planes and rods along ⟨100⟩. Still, the global short-range order scattering pattern indicates local order as the maximum is located at 0.6 0 0 and not at 000.

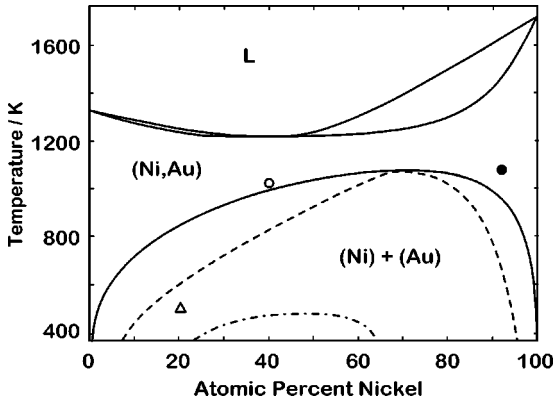

FIG. 1. Phase diagram according to Okamoto (Ref. 1). The symbols mark states investigated by (○) Wu and Cohen (Ref. 3), (●) the present authors, and (△) Renaud *et al.* (Ref. 8) (conditions before aging). Also shown is the chemical spinodal (dashed line) and the coherent spinodal (dash-dotted line) (Ref. 11).

Moss and Averbach[4] also investigated a Ni-60 at.% Au single crystal by diffuse x-ray scattering at room temperature in a 100 plane of reciprocal space and at small angles. Although an analysis in terms of short-range order parameters cannot be given from such a limited data set, an essentially random arrangement was noted for the sample rapidly quenched from 1163 K. No indication of local order was observed: local decomposition was considered plausible.

An explanation for the presence of short-range order was suggested by the *ab initio* electronic structure calculations of Wolverton *et al.*[7] The energy of alloy formation is separated into a ''spin-flip'' and a ''constituent-strain'' energy part. The latter part not only includes the large and positive energy of mixing but also lattice relaxation, and thus depends on direction and site occupation. This site-dependent part of the formation energy leads to local order as seen in the diffuse scattering,[3] and the total energy gives the global trend of alloy decomposition at low temperatures. This behavior was found to be robust when varying the Au content from 75 to 25 at.%.

A decisive item in these calculations was lattice relaxation (Fig. 11 of Ref. 7). Thus one might expect special features within the miscibility gap.[8,9] A metastable state of Ni-80 at.% Au (after a quench from 900 K and a subsequent aging at 520 K for 30 min) was investigated by Renaud *et al.*[8] using synchrotron radiation. This state is close to the coherent spinodal characterized as the temperature above which a modulated structure is no longer observed (the coherent spinodal was introduced for this alloy system by Golding and Moss;[10]

 ©2001 The American Physical Society

for a summary, see, e.g., Hofer and Warbichler[11]). The global maximum in the short-range order scattering was located at 0.4 0 0, for 000 a value between 0 and 1 Laue units was considered plausible. Values of the Warren-Cowley short-range order parameters similar to those of Wu and Cohen[3] were noted, a low positive value for α_{110} and a large positive value for α_{200}. However, Moss and Averbach[4] noted an increased small-angle scattering for slowly quenched Ni-60 at.% Au, i.e., an indication of decomposition.

For Ni-50 and -60 at.% Au, Zhao and Notis[9] demonstrated the possible existence of a transient long-range ordered state. The $L1_0$ structure was observed when annealing a specimen first at 473 K (below the coherent spinodal) for 8.3 h or 32 d and then in a transmission electron microscope *in situ* at 763 K (above the coherent spinodal). The ordered phase evolved at the interface between the precipitates and matrix or at the sample surface. Its formation was attributed to lattice relaxation.

To discuss the conflicting results of local order versus local decomposition for states above the miscibility gap, the favorable aspects of a diffuse neutron scattering experiment were not yet exploited (all previous diffuse scattering experiments employed x rays). Especially in decomposing alloys, it is difficult to separate static quadratic displacement scattering, thermal diffuse scattering of first order, and short-range order scattering because of a similar variation of the underlying Fourier series in reciprocal space. For an alloy with large atomic size mismatch, separation is achieved most reliably when using diffuse scattering within the first Brillouin zone [see, e.g., the discussion on Guinier-Preston zones in Al-rich Al-Cu (Ref. 13)]. Diffuse neutron scattering experiments provide easy access to this region and also benefit from the ease of experimentally separating thermal diffuse scattering (apart from regions close to Bragg reflections) from the elastic diffuse scattering contribution. In the case of Ni-Au, the large elastic incoherent scattering of natural Ni is easily suppressed by using, e.g., the Ni-58 isotope. Ni-rich alloys are more suited for diffuse neutron scattering experiments than Au-rich alloys because of the large absorption cross section of Au.

Another reason for studying a Ni-rich Ni-Au alloy is the prediction[7] of a maximum in short-range order scattering along the Γ-W line, a location not yet observed in any experiment. In a recent paper,[12] however, a maximum along the Γ-X line was considered possible for Ni-rich alloys.

II. THEORY

The elastic diffuse scattering I_{diff} from crystalline solid solutions originates from the mere presence of different scatterers and from static deviations of the actual atomic sites from those of the average lattice. The corresponding scattering terms are called short-range order scattering and displacement scattering. In contrast to short-range order scattering (I_{SRO}), displacement scattering cannot be represented in closed form and is commonly written as a series expansion (see, e.g., Schwartz and Cohen[14]). The leading terms are called size effect scattering (I_{SE}) and Huang scattering (I_{H}).

Short-range order scattering and size effect scattering [in Laue units, 1 L.u.$=c_A c_B(b_A-b_B)^2$ with c_μ=atomic fraction and b_μ=coherent scattering length of component μ] are given for a binary solid solution with cubic structure by

$$I_{\mathrm{SRO}}(\underline{h})=\sum_{lmn}\alpha_{lmn}\cos(\pi h_1 l)\cos(\pi h_2 m)\cos(\pi h_3 n), \tag{1}$$

$$I_{\mathrm{SE}}(\underline{h})=\sum_{i} h_i Q_i(\underline{h}), \tag{2}$$

where $\underline{h}=(h_1,h_2,h_3)$ is the scattering vector in reciprocal lattice units (r.l.u.) $2\pi/a$ (a=lattice parameter), the α_{lmn} are the Warren-Cowley short-range order parameters[15] for the *lmn*-type neighbors (l, m, n in units of $a/2$ representing the position), and, e.g.,

$$Q_1(\underline{h})=\sum_{lmn}\gamma^{x}_{lmn}\sin(\pi h_1 l)\cos(\pi h_2 m)\cos(\pi h_3 n). \tag{3}$$

For the representation of I_{H} as used in the present investigation, see Ref. 6. For a statistically uncorrelated arrangement of the elements, I_{SRO} is the monotonic Laue scattering. To recover short-range order scattering from the total diffuse scattering I_{diff}, several techniques have been developed. In the present case, least-squares fitting to the leading Fourier coefficients[16] was applied.

III. EXPERIMENT

An alloy of nominal composition Ni-10 at.% Au was prepared from 99.999+%gold (Métaux Précieux SA METALOR, Neuchâtel, Switzerland) and from isotopically pure (99.86 at.%) ^{58}Ni (State Scientific Centre, Moscow, Russia). From this alloy a single crystal was grown by the Bridgman technique. The cylindrically shaped sample used for the diffuse scattering experiments had a diameter and height of 8 mm and a cylinder axis near ⟨421⟩. The concentration as determined by x-ray fluorescence analysis was Ni-8.4(4) at.% Au; the error gives the standard deviation over 50 individual positions.

The diffuse scattering was measured on the triple-axis spectrometer DrüchaL (PSI, Villigen, Switzerland) equipped with a high-temperature furnace[17] and an Eulerian cradle. This setup gives access to a hemisphere of scattering vectors in the temperature range from 293 to 1400 K. The measurement was performed at 1083(5) K, about 100 K above the miscibility gap. Neutrons with an energy of 14.68(50) meV were used; the λ/n harmonics were suppressed to better than 10^{-3} by 10 cm of pyrolytic graphite. Typically, 300–3000 counts were registered under monitor control within 840 s at about 730 crystal settings within 0.2–2.1 r.l.u. These settings are located on a grid of 0.1 r.l.u. within a minimum volume for the separation of short-range order scattering and linear and quadratic displacement scattering. To get scattering data near the origin of reciprocal space, about 20 crystal settings within 0.13–0.60 r.l.u. were investigated using neutrons of 4.76(15) meV, suppressing the λ/n harmonics by a beryllium filter. With this energy the background scattering was re-

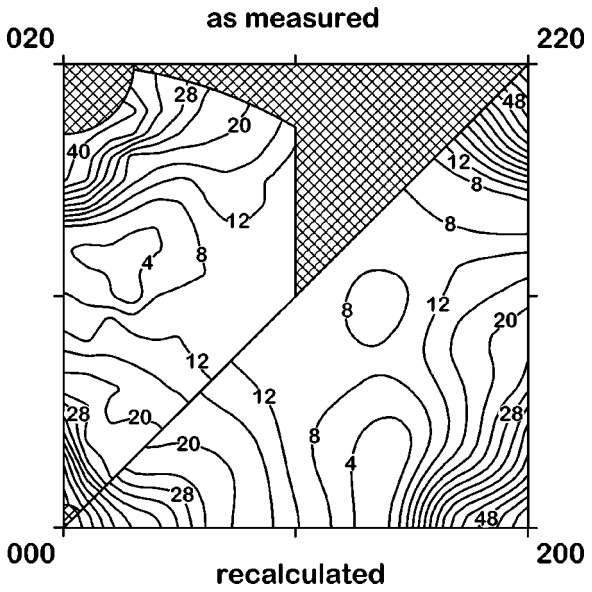

FIG. 2. The as-measured and recalculated elastic diffuse scattering (in 0.1 Laue units, uncorrected data) from ^{58}Ni-8.4 at. % Au at h_1h_20 positions.

duced by nearly a factor of 2. For both energies the scattering intensities were converted to absolute scattering cross sections using the elastic incoherent scattering of a vanadium sample with identical dimensions as the Ni-Au sample.

For both energies multiple scattering[18] and absorption were considered. An overall (static and dynamic) Debye-Waller factor[19] $\exp[-2B(\sin\theta/\lambda)^2]$ was calculated for Ni-8.4 at.% Au on the basis of the elastic constants $c_{11}=204$ GPa, $c_{12}=141$ GPa, and $c_{44}=89$ GPa estimated from Ref. 20. Values of $B_{\rm stat}=0.115\times10^{-2}$ nm^2 for the static part and $B_{\rm dyn}=1.481\times10^{-2}$ nm^2 for the dynamic part of B were obtained. For vanadium $B=0.485\times10^{-2}$ nm^2 was used.[21] The coherent scattering lengths $b_{^{58}\rm Ni}=14.4(1)$ fm and $b_{\rm Au}=7.63(6)$ fm, the incoherent scattering cross sections $\sigma^{\rm inc}_{^{58}\rm Ni}=0$ b, $\sigma^{\rm inc}_{\rm Au}=0.43(5)$ b, and $\sigma^{\rm inc}_{\rm V}=5.08(4)$ b were taken from Ref. 22.

IV. ELASTIC DIFFUSE SCATTERING

The measured elastic diffuse scattering from ^{58}Ni-8.4 at.% Au is shown in Fig. 2. The intensities measured at the incident neutron energies of 4.76 and 14.68 meV smoothly overlap and are treated as one data set without any scaling factor. A diffuse maximum is observed at 000. A region of 0.3 r.l.u. around each fundamental reflection was discarded in the subsequent data evaluation as it may contain contributions from thermal diffuse scattering. No sign for a static concentration wave along $\langle100\rangle$ is indicated between the fundamental reflections.

The elastic diffuse scattering was least-squares fitted with a set of Warren-Cowley short-range order parameters and linear and quadratic atomic displacement parameters. In addition, the scattering intensity at 000 was set equal to that at 0.13 0 0. Judging the quality of each fit from its weighted R value, a set of 13 α_{lmn}, 33 γ^x_{lmn}, and 9 $\delta^x_{lmn}/\epsilon^{xy}_{lmn}$ was finally used (Table I). The recalculated elastic diffuse scattering (Fig. 2) reproduces the experimental data within ±0.2 L.u., well within the standard deviation of 0.3 L.u. solely due to counting statistics.

TABLE I. Warren-Cowley short-range order parameters α_{lmn} of Ni-8.4 at.% Au at 1083 K using the uncorrected and corrected scattering intensities. The numbers in the brackets give the standard deviations due to counting statistics.

	α_{lmn}	
lmn	Uncorrected	Corrected
000	0.594(29)	0.970(41)
110	0.133(11)	0.174(10)
200	0.084(10)	0.099(13)
211	0.015(6)	0.034(6)
220	0.008(4)	0.013(4)
310	0.021(4)	0.023(4)
222	−0.007(4)	−0.008(5)
321	0.000(2)	−0.001(2)
400	0.013(4)	0.020(6)
330	−0.001(3)	−0.003(4)
411	0.009(2)	0.017(3)
420	0.006(2)	0.011(3)
233	−0.004(2)	−0.011(3)
422		−0.000(3)
431		−0.003(2)
510		0.016(3)
521		0.004(2)

For the Warren-Cowley short-range order parameter α_{000} a value of 0.59(3) is found, much smaller than the theoretical value of 1. Values smaller than 1 were repeatedly obtained from diffuse neutron scattering experiments at high temperatures: (i) 0.4 for Ni-V, 0.20–0.87 for Ni-Cr by Caudron *et al.*,[23] (ii) 0.85–0.99 for Pt-V and 0.78 for Ni-V by Le Bolloc'h,[24] and (iii) 0.595(5) for Ni-Ti by Bucher *et al.*[25] and 0.48–0.80 for Fe-Al by Bucher.[17] In comparison with these investigations where thermal diffuse scattering was always separated off experimentally, diffuse x-ray scattering experiments at high temperatures (using calculated thermal diffuse scattering) did not reveal a strong deviation of α_{000} from 1. Consistently, a diffuse neutron scattering experiment without energy resolution performed at 1033 K with the same Fe-Al sample as used by Ref. 17 yielded $\alpha_{000}=1.09(6)$. Based on these data of Fe-Al, a procedure was set up for the correction of the elastic diffuse scattering that essentially scales α_{000} to 1, multiplying the scattering intensities by a constant factor and adding a constant term to the scattering intensity. In the present case, a factor of 1.4 and an additive term of 0.2 L.u. were employed. This strategy lead to temperature independent effective pair interactions for Fe-Al.

A. Short-range order scattering

The least-squares fitting was performed with a set of 17 short-range order parameters, 18 linear, and 8 quadratic displacement parameters. The α_{lmn} for the corrected intensities

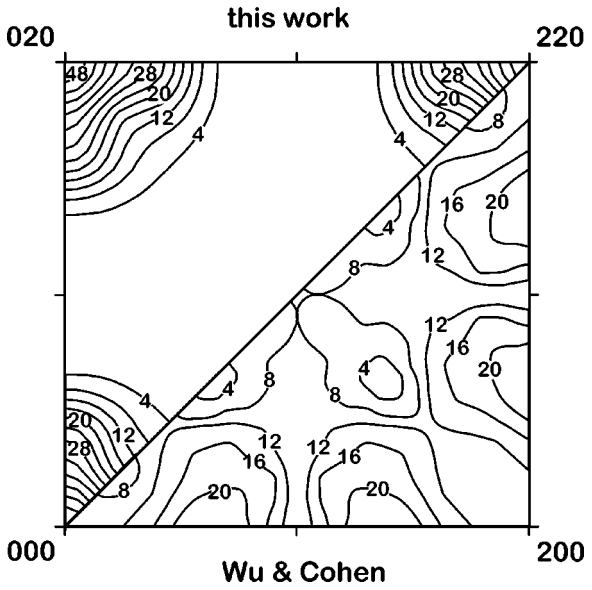

FIG. 3. Short-range order scattering I_{SRO} (in 0.1 Laue units) from ^{58}Ni-8.4 at. % Au (based on corrected scattering intensities) and from Ni-60 at. % Au (Ref. 3) at h_1h_20 positions.

are given in Table I. The dominating Fourier coefficient is $\alpha_{110}=0.17(1)$, positive as expected for a decomposing alloy system. The further $\alpha_{lmn\neq 000}$ are mostly positive. They approach zero smoothly and rapidly. The recalculated short-range order scattering is shown in Fig. 3. A strong maximum of about 5 L.u. is located at 000.

For comparison, the recalculated short-range order scattering of Ni-60 at.% Au (Ref. 3) is shown in Fig. 3, with a maximum of about 2.3 L.u. at 0.6 0 0. The largest discrepancy between both short-range order scattering patterns is noted for the region around 000. This coincides with the extended range of 0.45 r.l.u. around the fundamental reflections where Wu and Cohen[3] found it to be increasingly difficult to separate short-range order scattering from dynamic and static displacement scattering (as indicated by the large *R* value between the recalculated and measured diffuse scattering). As a consequence, the short-range order parameters of Wu and Cohen[3] strongly differ from the present result, with $\alpha_{200}=0.15(4)$ and $\alpha_{110}=0.04(5)$.

B. Displacement scattering

The atomic displacement parameters γ^x_{lmn} and $\delta^x_{lmn}/\epsilon^{xy}_{lmn}$ are summarized in Table II. Linear and quadratic displacement scattering (Fig. 4) are strongly modulated because of the large atomic size mismatch of 15% between Ni and Au. That is the reason why it is important to measure at small angles to obtain short-range order scattering in a decomposing system. The linear displacement scattering is antisymmetric around the fundamental reflections with positive contributions at the side of larger $|\underline{h}|$ values. Such an intensity distribution is found if the atom with the smaller coherent scattering length (Au) has the larger atomic size.

With the species-dependent linear displacement parameters of Wu and Cohen[3] the γ^x_{lmn} for alloys with a different composition and comparable heat treatment may be estimated. For the first two shells of neighbors, $\gamma^x_{110}=4.75$ and $\gamma^x_{200}=-8.37$ are obtained for Ni-8.4 at.% Au at 1083 K. These values are by one to two orders of magnitude larger than those given in Table II. Also, the values of the subsequent shells are much larger. In previous comparisons of linear displacement parameters obtained with neutrons and (species dependent) with x rays (Ni-rich Ni-Al in Ref. 26 and Ni-Cr in Ref. 27), good agreement was found. A strong compositional dependence could be the reason for the discrepancy in the present case.

TABLE II. Linear (γ^x_{lmn}) and quadratic (δ^x_{lmn} and ϵ^{xy}_{lmn}) displacement parameters determined from the corrected elastic diffuse scattering.

lmn	γ^x_{lmn}	*lmn*	δ^x_{lmn}	ϵ^{xy}_{lmn}
110	0.182(10)	000	0.326(21)	
200	−0.081(11)	110	−0.035(5)	−0.062(11)
211	−0.021(6)	011	0.054(7)	
121	−0.011(3)	200	−0.051(11)	
220	−0.012(5)	020	−0.009(7)	
310	−0.022(6)	211	−0.022(5)	
130	−0.017(5)	121	0.004(3)	
222	−0.008(4)			
321	0.001(4)			
231	−0.005(4)			
123	−0.002(3)			
400	−0.010(10)			
330	0.003(4)			
411	−0.003(5)			
141	0.000(3)			
420	−0.006(4)			
240	0.001(4)			
233	0.010(4)			

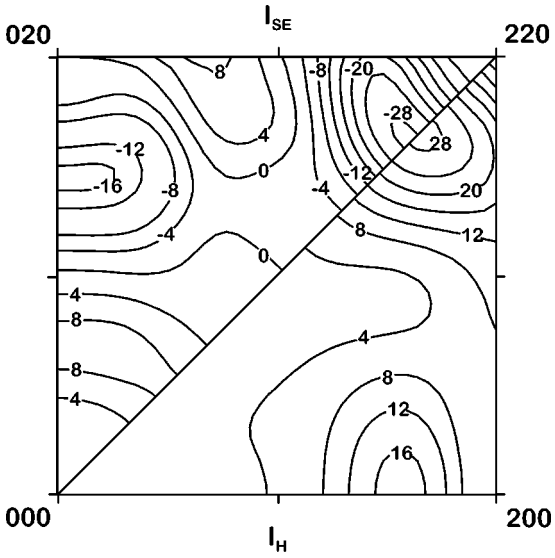

FIG. 4. Size effect scattering I_{SE} and Huang scattering I_{H} (both in 0.1 Laue units) from ^{58}Ni-8.4 at. % Au at h_1h_20 positions.

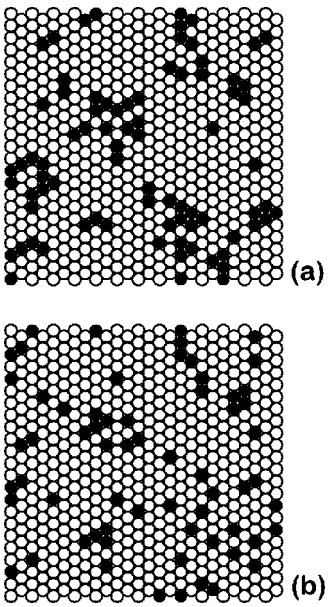

FIG. 5. A {111} plane of ^{58}Ni-8.4 at. % Au at 1083 K (a). For comparison, a {111} plane of a statistically uncorrelated arrangement of the same composition is shown (open circles, Ni atoms; solid circles, Au atoms).

V. MODELING

Based on the corrected Warren-Cowley short-range order parameters (Table I), crystals of $32\times32\times32$ fcc unit cells were modeled using the procedure introduced by Gehlen and Cohen.[28] Starting from a random arrangement and exchanging randomly chosen Ni and Au atoms, the α_{lmn} calculated for the final modeled crystals lie within the statistical error bars of the experimental data. The difference between a statistically uncorrelated arrangement and a short-range decomposed model crystal is illustrated in Fig. 5. Small groups of minority atoms (Au) on {111} planes are typical for the short-range decomposed state.

For a quantitative analysis all nearest-neighbor configurations (Clapp configurations; for its nomenclature, see Clapp[29]) were searched. Results for enhancement factors (ratios of the numbers of the same configurations present in the short-range ordered and in the random crystals) and abundances were obtained by averaging over five short-range decomposed and five random crystals (Table III). Two cases were considered.

(i) The possible superstructures $L1_2$ and $L1_0$ (Ref. 9) are characterized by the configurations $C16$, chosing the cases of minority atoms (Au) around any majority atom (Ni) for $L1_2$ and minority atoms (Au) around any minority atom (Au) for $L1_0$. As Ni-8.4 at.% Au contains less than the 25% or 50% minority atoms of these superstructures, minority atoms must be replaced by majority atoms. This gives the sequences $C16\rightarrow C7\rightarrow C3$, $C4$. As all the characteristic configurations of $L1_2$ have enhancement factors less than 1, $L1_2$ is not a plausible (metastable) superstructure. On the other hand, enhancement factors larger than one are found for the characteristic configurations of $L1_0$. Zhao and Notis[9] also found $L1_0$ as a plausible superstructure of a metastable state.

TABLE III. Abundances and enhancement factors of ^{58}Ni-8.4 at.% Au alloy at 1083 K with respect to a statistically uncorelated arrangement for selected Clapp configurations (considering Au around Ni for the $L1_2$ structure, Au around Au for the $L1_0$ structure and for decomposition).

Clapp configuration	Enhancement factor	Abundance in %
Au around Ni		
$C16$	0.7	0.01
$C7$	0.4	0.12
$C3/C4$	0.4	2.25
Au around Au		
$C16$	5.0	0.05
$C7$	1.9	0.57
$C3/C4$	1.1	4.71
Au around Au		
$C33$	96.1	5.2
$C31$	32.2	2.6
$C15$	15.5	2.8
$C13$	9.1	5.8
$C14$	6.2	3.6

(ii) For the characterization of Au agglomerates, only the configurations of minority atoms around minority atoms with abundances larger than 2% and largest enhancement factors are summarized in Table III. The most important configuration $C33$ is a tetrahedron ($C15$) plus an adjacent atom as indicated by the Au agglomerates on {111} planes in Fig. 5.

VI. POTENTIALS

From the set of α_{lmn} of Table I, effective pair interaction parameters V_{lmn} were determined by the inverse Monte Carlo method.[30] In the case of a canonical ensemble and binary *A-B* alloy, the ordering energy is

$$H/N = c_A c_B \sum_{lmn} \alpha_{lmn} V_{lmn}, \tag{4}$$

with $V_{lmn}=\frac{1}{2}(V_{lmn}^{AA}+V_{lmn}^{BB})-V_{lmn}^{AB}$ and N the number of atoms. They were deduced from 200 000 virtual exchanges of modeled short-range decomposed crystals with $32\times32\times32$ fcc unit cells employing linear boundary conditions. The V_{lmn} were subsequently used in Monte Carlo simulations to recalculate the Warren-Cowley short-range order parameters $\alpha_{lmn}^{\mathrm{rec}}$. At least, seven V_{lmn} are required as judged from the value of $R_\alpha=\Sigma_{lmn}|\alpha_{lmn}-\alpha_{lmn}^{\mathrm{rec}}|/\Sigma_{lmn}|\alpha_{lmn}|$. The values and standard deviations given in Table IV refer to five model crystals. The V_{lmn} for the first two neighbor shells are negative as expected for a decomposing alloy system. From the standard deviation, just the first four were found to be statistically relevant.

At the 100 position no local minimum in $V(\underline{k})=\Sigma_{lmn}V_{lmn}e^{i\underline{k}\cdot\underline{r}_{lmn}}$ is seen. Its presence would corroborate the metastable $L1_0$ structure found in Ref. 9, following the reasoning of Reinhard and Turchi.[31] These authors inter-

TABLE IV. Effective pair interaction parameters V_{lmn} as obtained by the inverse Monte Carlo method using the corrected α_{lmn} of Table I.

lmn	V_{lmn} (meV)
110	−37.9(60)
200	−19.4(79)
211	4.7(33)
220	8.0(47)
310	0.2(32)
222	3.2(31)
321	1.4(24)

preted a local minimum in $V(\underline{k})$ of Ti-V as an indicator for transient ordering in the low-temperature region.

VII. DISCUSSION

The main result of the present study is that short-range decomposition and not short-range order is observed for Ni-8.4 at.% Au above the miscibility gap. An increase in the diffuse scattering towards 000 was demonstrated using diffuse neutron scattering. This result is at variance with the results of almost all diffuse x-ray scattering studies of Ni-Au at temperature,[2,3] of alloys quenched from the solid solution,[2] or even of an alloy aged within the two-phase state.[8] The only exception is the decomposition nature in the short-range order scattering as evaluated by Borie and Sparks using data of Moss and Averbach (Fig. 7 of Ref. 4).

The generally different conclusions on the local atomic arrangement in previous studies may have been reached because diffuse scattering was never measured at sufficiently small angles. One might further argue that the only detailed investigation at high temperature by Wu and Cohen[3] was performed for an alloy with a much larger Au fraction. Diffuse neutron scattering at smaller angles should also be measured for a ^{58}Ni-60 at.% Au single crystal. From the electronic-structure calculations of Wolverton *et al.*,[7] short-range order is expected for a broad range of compositions. The question on the compositional modulation either along $\langle 100\rangle$ or $\langle 1\frac{1}{2}0\rangle$ on the Ni-rich side[12] could not be answered as no such modulations were seen at all. Maybe, they will be revealed after aging within the miscibility gap.

According to Chakraborty,[32] the *A-B* nearest-neighbor distance of an *A-B* alloy should be larger than the arithmetic mean of the *A-A* and *B-B* distances for short-range decomposed alloys, but smaller for short-range ordered alloys. The displacement parameters of Wu and Cohen[3] fulfill the criterion that the state investigated be short-range decomposed (in contrast to the I_{SRO} pattern in Ref. 3), while the metastable states investigated by Renaud *et al.*[33] using extended x-ray absorption fine structure (EXAFS) fulfill the criterion of short-range order (in agreement with the I_{SRO} pattern in Ref. 8). More information of the species-dependent static atomic displacements is thus required for Ni-Au. For the present composition of Ni-8.4 at.% Au they may be obtained if one performs a second diffuse scattering experiment employing the Ni-60 instead of the Ni-58 isotope.

Asta and Foiles[34] compared Ni-Au with two other alloy systems, Ni-Cu and Ag-Cu, which also show a large two-phase region over the whole range of composition. In their electronic-structure calculations, Asta and Folies[34] distinguished two cases: effective pair interaction parameters with (i) chemical and relaxation-energy contributions and (ii) only comprising chemical contributions. For Ni-Cu with a small size misfit of 2.5%, the nearest-neighbor parameter is negative in both cases, consistent with diffuse neutron scattering experiments on samples quenched from above the miscibility gap.[35–37] For Ni-Au (and Ag-Cu) a change in sign is found between both cases; a negative sign is obtained if both contributions are considered. Thus only case (ii) is consistent with the results of the present investigation. Consequently, in contrast to Ref. 7, no problems arise in determining effective pair interaction parameters from diffuse scattering above the miscibility gap.

ACKNOWLEDGMENTS

The authors thank E. Fischer very much for growing the single crystal. Financial support by the Swiss National Science Foundation is gratefully acknowledged.

[1] H. Okamoto, in *Phase Diagrams of Binary Gold Alloys*, edited by H. Okamoto and T. B. Massalski (ASM International, Materials Park, OH, 1987), p. 193.
[2] P. A. Flinn, B. L. Averbach, and M. Cohen, Acta Metall. **1**, 664 (1953).
[3] T. B. Wu and J. B. Cohen, Acta Metall. **31**, 1929 (1983).
[4] S. C. Moss and B. L. Averbach, in *Small-angle X-ray Scattering*, edited by H. Brumberger (Gordon and Breach, New York, 1967), p. 335.
[5] G. Kostorz, in *Physical Metallurgy*, 4th ed., edited by R. W. Cahn and P. Haasen (North-Holland, Amsterdam, 1996), p. 1115.
[6] B. Schönfeld, Prog. Mater. Sci. **44**, 435 (1999).
[7] C. Wolverton, V. Ozolins, and A. Zunger, Phys. Rev. B **57**, 4332 (1998).
[8] G. Renaud, M. Belakhovsky, S. Lefebvre, and M. Bessière, J. Phys. III **5**, 1391 (1995).
[9] J.-C. Zhao and A. Notis, Metall. Mater. Trans. A **30**, 707 (1999).
[10] B. Golding and S. C. Moss, Acta Metall. **15**, 1239 (1967).
[11] F. Hofer and P. Warbichler, Z. Metallkd. **76**, 11 (1985).
[12] C. Wolverton, V. Ozolins, and A. Zunger, J. Phys.: Condens. Matter **12**, 2749 (1999).
[13] V. Gerold, Scr. Metall. **22**, 927 (1988) and subsequent papers (Viewpoint Set No. 13).
[14] L. H. Schwartz and J. B. Cohen, *Diffraction from Materials* (Springer, Berlin, 1987).
[15] J. M. Cowley, J. Appl. Phys. **21**, 24 (1950).
[16] R. O. Williams (unpublished).
[17] R. Bucher, Ph.D. thesis, ETH Zürich, 1999.

[18] V. F. Sears, Adv. Phys. **24**, 1 (1975).
[19] M. A. Krivoglaz, *X-ray and Neutron Diffraction in Nonideal Crystals* (Springer, Berlin, 1996).
[20] G. A. Alers, J. R. Neighbours, and H. Sato, Phys. Chem. Solids **13**, 40 (1960); J. R. Neighbours and G. A. Alers, Phys. Rev. **111**, 707 (1958).
[21] R. Colella and B. W. Batterman, Phys. Rev. B **1**, 3913 (1970).
[22] V. F. Sears, Neutron News **3**, 26 (1992).
[23] R. Caudron, M. Sarfati, M. Barrachin, A. Finel, F. Ducastelle, and F. Solal, J. Phys. I **2**, 1145 (1992).
[24] D. Le Bolloc'h, Ph.D. thesis, Université Rennes, 1997.
[25] R. Bucher, B. Schönfeld, G. Kostorz, and M. Zolliker, Phys. Status Solidi A **175**, 527 (1999).
[26] B. Schönfeld, L. Reinhard, G. Kostorz, and W. Bührer, Acta Mater. **45**, 5187 (1997).
[27] B. Schönfeld, G. E. Ice, C. J. Sparks, H.-G. Haubold, W. Schweika, and L. B. Shaffer, Phys. Status Solidi B **183**, 79 (1994).
[28] P. C. Gehlen and J. B. Cohen, Phys. Rev. **139**, A844 (1965).
[29] P. C. Clapp, Phys. Rev. B **4**, 255 (1971).
[30] V. Gerold and J. Kern, Acta Metall. **35**, 393 (1987).
[31] L. Reinhard and P. E. A. Turchi, Phys. Rev. Lett. **72**, 120 (1994).
[32] B. Chakraborty, Europhys. Lett. **30**, 531 (1995).
[33] G. Renaud, N. Motta, F. Lancon, and M. Belakhovsky, Phys. Rev. B **38**, 5944 (1988).
[34] M. Asta and S. M. Foiles, Phys. Rev. B **53**, 2389 (1996).
[35] B. Mozer, D. T. Keating, and S. C. Moss, Phys. Rev. **175**, 868 (1968).
[36] J. Vrijen and S. Radelaar, Phys. Rev. B **17**, 409 (1978).
[37] W. Wagner, R. Poerschke, A. Axmann, and D. Schwahn, Phys. Rev. B **21**, 3087 (1980).